Chinese Chemical Letters 34 (2023) 107134

Contents lists available at ScienceDirect

Chinese Chemical Letters

journal homepage: www.elsevier.com/locate/cclet

Ultrathin two-dimensional triptycence-based metal-organic framework for highly selective CO_2 electroreduction to CO

Huan Xue[1], Haolin Zhu[1], Jiarun Huang, Peiqin Liao*, Xiaoming Chen

MOE Key Laboratory of Bioinorganic and Synthetic Chemistry, School of Chemistry, Sun Yat-sen University, Guangzhou 510275, China

ARTICLE INFO

Article history:
Received 30 November 2021
Revised 3 January 2022
Accepted 10 January 2022
Available online 16 January 2022

Keywords:
Triptycence
Metal organic framework
Nanosheet
Electrochemical CO_2 reduction
Carbon monoxide production

ABSTRACT

Efficient CO_2 reduction reaction (CO_2RR) is one of the important topics in energy and environment field, but improving the electrochemical selectivity of specific product is a great challenge. Herein, we reported a unprecedented two-dimensional (2D) metal–organic framework with CuO_4 unit (denoted as Cu-HHTT, HHTT = 9,10-dihydro-9,10-[1,2]benzenoanthracene-2,3,6,7,14,15-hexaol) as the electrocatalyst for CO_2RR. Cu-HHTT exhibits high performance for CO_2RR to produce CO, namely Faradaic efficiency of 96.6% toward CO with a current density of 18 mA/cm^2 at the potential of −0.6 V *vs.* RHE. Density function theory reveals that the desorption of CO species exhibits a lower energy barrier than that of hydrogenation of *CO intermediate, resulting in CO as the main product instead of alcohols or hydrocarbons.

As a novel and effective way for yielding fuels, electrochemical carbon dioxide reduction reaction (CO_2RR) attracts much attention because it is a promising method to kill two birds with one stone to solve environmental problems and energy crisis [1–9]. Beneficial from the designable frameworks and abundant active sites, metal-organic frameworks (MOFs) are regarded as a series of good candidate for electrochemical CO_2RR [2]. However, the complexity of control conditions for the lattice planes and the insufficient exposure of metal sites of MOFs restrict their industrial and commercial application in electrochemical CO_2RR. Since the first report of single-layer graphene, two-dimensional (2D) materials have been proved to have tunable exposed lattice planes and unique electronic states [10,11]. Therefore, compared to those of the three-dimensional MOFs, the specific lattice planes and metal sites of 2D-MOFs are easier to be exposed through reasonable design, which endows 2D-MOFs with more potential for electrochemical CO_2RR. Generally, two types of 2D-MOFs usually serve as electrocatalysts for CO_2RR, namely hexahydroxy-aromatic MOFs and phthalocyanine-based MOFs [2,6,12,13]. For example, 2D Cu-THQ [14] (THQ = tetrahydroxyquinone) and Cu_2O@Cu-HHTP [15] (HHTP = 2,3,6,7,10,11-hexahydroxytriphenylene) revealed a Faradaic efficiency (FE) of 91% toward CO and a FE of 73% toward CH_4, respectively. Recently, we reported a Cu phthalocyanine-based MOF (PcCu-Cu-O) as an electrocatalyst producing C_2H_4 with a FE of 50% [2]. However, there are only a few reports on 2D-MOFs as electrocatalysts for CO_2RR. More 2D-MOFs remain to be developed as electrocatalyst for CO_2RR.

Currently, several types of products have been obtained through electrochemical CO_2RR, including carbon monoxide (CO) [6,14,16,17], hydrocarbons [2,15,18], carboxylic acid [19,20] and alcohols [21]. Taking market prices of these products as well as the cost of electricity into account, CO and formic acid are the most promising products for industrial application [22]. According to previous reports, 2D MOFs with CuO_4 secondary building units tend to exhibit high selectivity toward CO [14,15].

Combining the advantages of 2D structures and CuO_4 unit, herein, for the first time, we designed and synthesized a triphene-based MOF nanosheet, $Cu_3(HHTT)_2$ (Cu-HHTT, HHTT = 9,10-dihydro-9,10-[1,2]benzenoanthracene-2,3,6,7,14,15-hexaol) *via* the solvothermal treatment (Fig. 1). Powder X-ray diffraction (PXRD) pattern of the obtained Cu-HHTT commendably match the simulated one (Fig. S1 in Supporting information), indicative of the successful preparation of Cu-HHTT. Cu-HHTT exhibits an AAA inclined packing (Fig. 1b). The shortest distance between the oxygen atoms of CuO_4 units and the aromatic hydrogen atoms is 3.14 Å, indicative of the existence of interlaminar hydrogen bonds (Fig. S2 in Supporting information), which assist to improve the framework stability. The disappearance of the hydroxyl peak in Fourier Transform Infrared (FTIR) spectrum of Cu-HHTT in contrast to that of HHTT suggests the successful synthesis of Cu-HHTT (Fig. S3 in Supporting information). Thermogravimetric curve of Cu-HHTT indicates a thermal stability up to 160 °C (Fig. S4 in Supporting information). X-ray photoelectron spectroscopy (XPS) spectra reveals a mixed-valence state of the as-synthesized Cu-HHTT (Fig. 2a). As is demonstrated by transmission electronic

* Corresponding author.
E-mail address: liaopq3@mail.sysu.edu.cn (P. Liao).
[1] These authors contributed equally to this work.

https://doi.org/10.1016/j.cclet.2022.01.027
1001-8417/

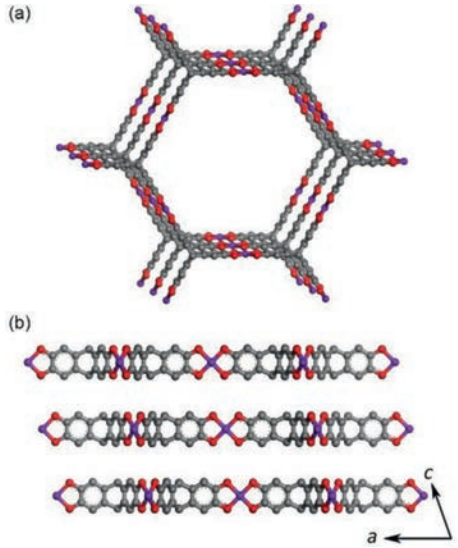

Fig. 1. (a) 2D layers of Cu-HHTT viewing along the *c*-axis and (b) the *b*-axis. Color code: Cu, purple; C, gray; O, red. Hydrogen atoms are omitted for clarity.

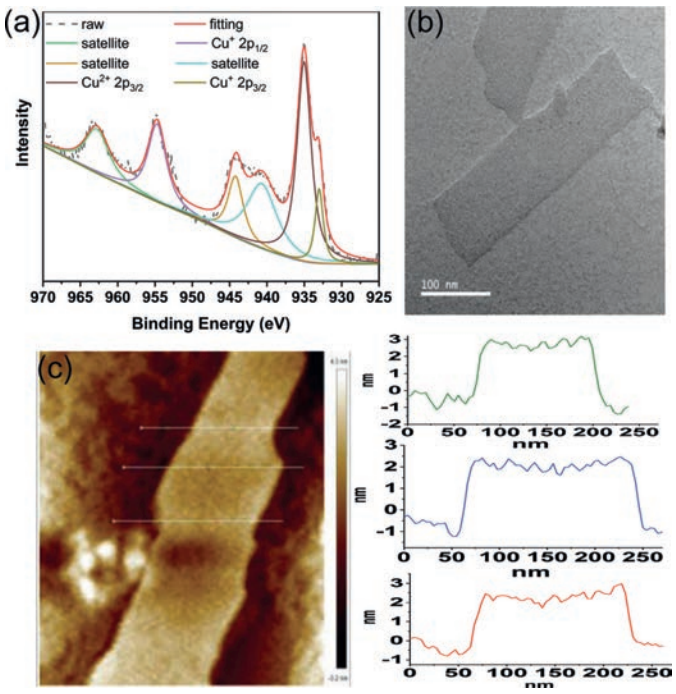

Fig. 2. (a) Cu 2p spectra, (b) TEM image and (c) AFM image of Cu-HHTT.

microscope (TEM) and atomic force microscope (AFM), Cu-HHTT exhibits morphology of the ultrathin nanosheet with the thickness of 2.90 ± 0.22 Å (Figs. 2b and c, Fig. S5 in Supporting information). As been demonstrated in our previous work that, in contrast to bulk MOFs, MOF nanosheets can exhibit enhanced electrochemical CO_2RR performances [2]. Compared with the general hexahydroxy-aromatic MOFs and phthalocyanine-based MOFs, the Cu ions in Cu-HHTT are located on the channel wall, causing more exposure of the potential active sites to the environmental media, which might exhibit high performance of electrochemical CO_2RR to CO.

In order to examine the affinity of Cu-HHTT to CO_2, we performed CO_2 adsorption measurements. The activated Cu-HHTT exhibits a saturation uptake of 136.39 cm^3/g toward CO_2 at 195 K and 1 bar (Fig. S6 in Supporting information). Since the CO_2 uptake of most MOFs are 20–100 cm^3/g, we anticipate that Cu-HHTT exhibits more affinity to CO_2, indicative of a potential activity for electrochemical CO_2RR. Electrochemical measurements of Cu-HHTT were subsequently performed. According to cyclic voltammetry (CV) curves, Cu-HHTT exhibits a higher current density in CO_2-saturated solution than that in Ar-saturated solution (Fig. 3a), suggesting the existence of electrochemical CO_2RR, which is also corroborated by the apparent positive shift of onset potential of the linear cyclic voltammetry (LSV) curve recorded in CO_2-saturated electrolyte compared to that recorded in Ar-saturated electrolyte (Fig. 3b). An impressive Faradaic efficiency (FE) of 96.6% and a turnover frequency (TOF) of 7.3 s^{-1} toward CO with a current density of 18 mA/cm^2 of Cu-HHTT at the potential of −0.6 V *vs.* RHE (Figs. 3a-d) were observed. No liquid product was observed in ^1H nuclear magnetic resonance (NMR) spectra before and after the electrocatalysis (Fig. S7 in Supporting information). The electrochemical performance of Cu-HHTT surpasses most MOF-based electrocatalysts (Table S1 in Supporting information) [6,14,16,23-27]. Actually, to our best knowledge, it is the highest selectivity toward CO among all the Cu-MOF electrocatalysts.

For the evaluation the electrochemical durability, Cu-HHTT was applied with continuous potential of −0.6 V *vs.* RHE for at least 4 h. Almost no current attenuation was observed during the long-time durability evaluation (Fig. S8 in Supporting information), and after that, the FE value for CO product slightly decreased to 91.3%. The slight decrease in performance may be ascribed to the minor sloughing of the catalyst from the electrode. According to PXRD patterns and TEM images, no Cu, Cu_2O, or CuO clusters were observed after electrochemical CO_2RR (Figs. S9 and S10 in Supporting information). The XPS spectra of Cu-HHTT indicate that electrochemical CO_2RR causes negligible changes of the electrocatalyst (Fig. 2a and Fig. S11 in Supporting information).

As is illustrated in the literatures, the mechanism of electroreduction of CO_2 to CO generally involves the *COOH and *CO intermediates [22]. To capture the information of intermediates during CO_2RR, the attenuated total reflection Fourier transform infrared spectroscopy (ATR-FTIR) measurements were carried out (Fig. 4a). As a result, the peak at 1222 cm^{-1} corresponds to the C–O stretch-

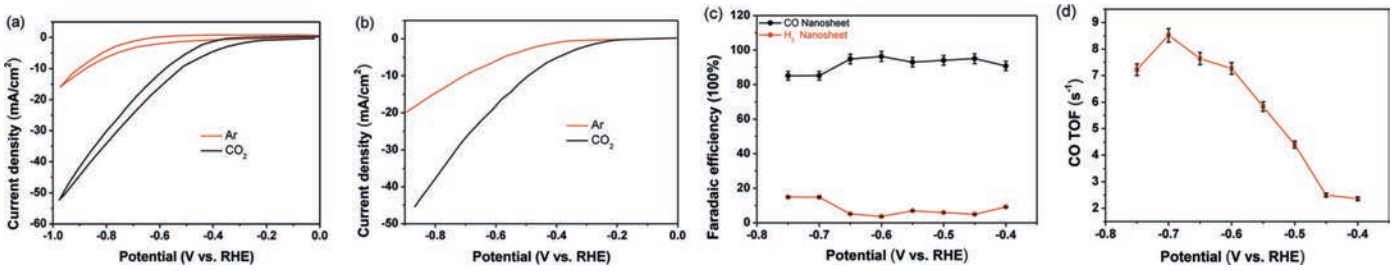

Fig. 3. (a) Cyclic voltammetry curves and (b) LSV curves of Cu-HHTT in Ar- and CO_2-saturated 0.1 mol/L $KHCO_3$ electrolyte. (c) Faradaic efficiencies of CO and H_2 for Cu-HHTT. (d) Turnover frequency for Cu-HHTT.

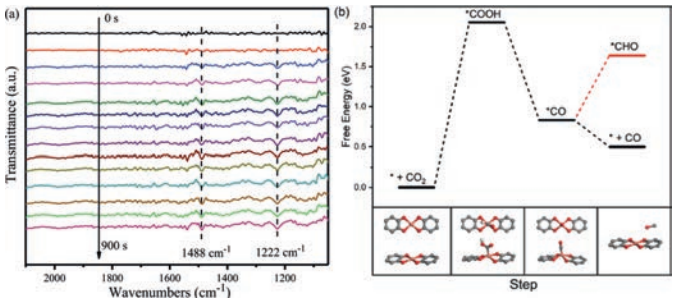

Fig. 4. (a) *In-situ* ATR-FTIR spectra of electrochemical CO_2RR on Cu-HHTT. (b) Free energy diagrams for the conversion of CO_2 into CO on Cu-HHTT and the optimized structure of each intermediate.

ing in *COOH [2]. The absorption peak at 1488 cm^{-1} can be attributed to the symmetric vibration of *COOH intermediate. To further determine the reaction pathway, density functional theory (DFT) was employed to determine the reaction free energy. The changes of free energy for the desorption of CO and hydrogenation of *CO intermediate are −0.33 and 0.81 eV, respectively (Fig. 4b). Therefore, the generation of CO takes precedence of alcohols and/or alkanes, which coincides perfectly with the high selectivity toward CO obtained in the electrochemical measurements.

In summary, a 2D MOF Cu-HHTT with CuO_4 unit was successfully designed and synthesized for the first time. Its ultrathin nanosheet exhibits an impressive selectivity for electrochemical CO_2RR for yielding CO. The exposed CuO_4 sites and ultrathin nanosheet morphology play an important role in the excellent performance. This work proposes a new strategy to design 2D MOFs for the industrial conversion of CO_2 into CO.

Declaration of competing interest

The authors declare no conflict of interest.

Acknowledgments

This work was supported by the National Natural Science Foundation of China (NSFC, Nos. 21890380 and 21821003), Local Innovative and Research Teams Project of Guangdong Pearl River Talents Program (No. 2017BT01C161), Science and Technology Key Project of Guangdong Province, China (No. 2020B010188002), Guangzhou Science and Technology Project (No. 202002030291), and Guangdong Natural Science Funds for Distinguished Young Scholar (No. 2018B030306009).

Supplementary materials

Supplementary material associated with this article can be found, in the online version, at doi:10.1016/j.cclet.2022.01.027.

References

[1] D.H. Nam, O.S. Bushuyev, J. Li, P. De Luna, et al., J. Am. Chem. Soc. 140 (2018) 11378–11386.
[2] X.F. Qiu, H.L. Zhu, J.R. Huang, et al., J. Am. Chem. Soc. 143 (2021) 7242–7246.
[3] F. Yang, A. Chen, P.L. Deng, et al., Chem. Sci. 10 (2019) 7975–7981.
[4] X. Zhou, J. Dong, Y. Zhu, et al., J. Am. Chem. Soc. 143 (2021) 6681–6690.
[5] T. Chen, J.H. Dou, L. Yang, et al., J. Am. Chem. Soc. 142 (2020) 12367–12373.
[6] J.D. Yi, D.H. Si, R. Xie, et al., Angew. Chem. Int. Ed. 60 (2021) 17108–17114.
[7] P. An, L. Wei, H. Li, et al., J. Mater. Chem. A 8 (2020) 15936–15941.
[8] K. Chen, M. Cao, Y. Lin, et al., Adv. Funct. Mater. 31 (2021) 2111322.
[9] Q. Wang, K. Liu, J. Fu, et al., Angew. Chem. Int. Ed. 60 (2021) 25241–25245.
[10] H. Jin, C. Guo, X. Liu, et al., Chem. Rev. 118 (2018) 6337–6408.
[11] J. Liu, C. Guo, A. Vasileff, S. Qiao, Small Methods 1 (2017) 1600006.
[12] J. Liu, D. Yang, Y. Zhou, et al., Angew. Chem. Int. Ed. 60 (2021) 14473–14479.
[13] Y. Liu, S. Li, L. Dai, et al., Angew. Chem. Int. Ed. 60 (2021) 16409–16415.
[14] L. Majidi, A. Ahmadiparidari, N. Shan, et al., Adv. Mater. 33 (2021) 2004393.
[15] J.D. Yi, R. Xie, Z.L. Xie, et al., Angew. Chem. Int. Ed. 59 (2020) 23641–23648.
[16] M.D. Zhang, D.H. Si, J.D. Yi, et al., Sci. China Chem. 64 (2021) 1332–1339.
[17] H. Zhong, M. Ghorbani-Asl, K.H. Ly, et al., Nat. Commun. 11 (2020) 1409.
[18] Z. Meng, J. Luo, W. Li, K.A. Mirica, J. Am. Chem. Soc. 142 (2020) 21656–21669.
[19] X. Kang, L. Li, A. Sheveleva, et al., Nat. Commun. 11 (2020) 5464.
[20] X. Kang, B. Wang, K. Hu, et al., J. Am. Chem. Soc. 142 (2020) 17384–17392.
[21] Y. Wu, Z. Jiang, X. Lu, Y. Liang, H. Wang, Nature 575 (2019) 639–642.
[22] S. Jin, Z. Hao, K. Zhang, Z. Yan, J. Chen, Angew. Chem. Int. Ed. 60 (2021) 20627–20648.
[23] L. Ye, J. Liu, Y. Gao, et al., J. Mater. Chem. A 4 (2016) 15320–15326.
[24] Y. Guo, W. Shi, H. Yang, et al., J. Am. Chem. Soc. 141 (2019) 17875–17883.
[25] B.X. Dong, S.L. Qian, F.Y. Bu, et al., ACS Appl. Energy Mater. 1 (2018) 4662–4669.
[26] X. Jiang, H. Li, J. Xiao, et al., Nano Energy 52 (2018) 345–350.
[27] N. Kornienko, Y. Zhao, C.S. Kley, et al., J. Am. Chem. Soc. 137 (2015) 14129–14135.